# Measurements of double differential heavy particles production cross sections for 70 MeV protons

M. Hagiwara, T. Oishi, M. Baba,
*Cyclotron and Radioisotope Center, Tohoku University*
E-mail: *hagi@cyric.tohoku,ac,jp*
T. Sanami
*High Energy Accelerator Research Organization (KEK)*
M. Takada
*National Institute of Radiological Sciences*

Measurements of differential fragment production cross sections for proton-induced reaction are described. Double-differential fragment production cross sections for carbon and aluminum induced by 70 MeV protons were obtained with a specially designed Bragg curve spectrometer (BCS) and energy-time-of-flight method (E-TOF). The present data obtained with two different methods are consistent with each other and compared with other experiment and calculations, and showed systematic trend.

## 1. INTRODUCTION

Fragments which are secondary particles heavier than alpha-particles cause a large local ionization. It is a serious problem for a semiconductor device and human in space environment. For dosimetry and the evaluation of radiation effects in devices or instruments such as single event upset (SEU) by cosmic rays, the energy and angular doubly differential fragments production cross-section data (DDX) are required. Up to now, however, experimental data of the fragment production are very scarce due to experimental difficulties in fragment detection. Thus, almost all past experimental data on fragment production were obtained by the activation method that did not provide energy and angle information. Furthermore, theoretical calculation treating fragment production is very few. Therefore, it is important to accumulate reliable experimental DDX data for fragment production.

For fragment detection, we adopted 1) a Bragg curve spectrometer (BCS) [1,2] providing various information with a single counter and 2) an energy-time of fight (E-TOF) method [3] having the capability of mass identification even in the energy region where BCS is not applicable, while the solid angle is very small. For 1), BCS was designed with special care to apply to a neutron beam, in addition to a charged particle beam and resulted in success to obtain light fragments by proton- and neutron-induced reactions [4, 5]. BCS proved very promising for fragments detection even in neutron-induced reaction, while there are still some problems that should be solved. For 2), we have succeeded in the identification of the fragment up to mass number 12 emitted from carbon bombarded with 70 MeV protons. An E-TOF method can applied only to charged particle-induced reactions due to a small detector solid-angle, but the dynamic range of fragment energy is higher than in BCS.

This paper describes energy-angular fragment production measurements in proton-induced reaction with BCS and E-TOF method. The data obtained with both methods were complementary with each other. The data were compared with other experimental data and calculations.

## 2. BRAGG CURVE SPECTROMETER (BCS)

The details of Bragg curve spectrometer (BCS) developed are described in the previous report [4]. Figure

1 shows a schematic diagram of BCS. It is a cylindrical gridded ionization chamber (GIC) [6, 7] filled with an Ar + 10%$CH_4$ gas at a pressure of ~200 Torr. In the case of proton induced reaction, fragments produced from targets in the vacuum chamber enter the detector along the axis through a thin film window and ionize the gas in BCS. The free electrons drift to the anode by the electric field keeping a shape of the Bragg curve. The time distribution of the anode signal corresponds to the reversal of the ionization distribution (Bragg curve) by the fragment. Therefore the fast part of anode signal is proportional to the Bragg peak value that is in proportion to the atomic number (Z) of the fragment. The integration of the whole anode signal represents the total charge that is proportional to the fragment energy. Therefore, BCS can provide information on the energy and the atomic number of fragments using only the anode signal.

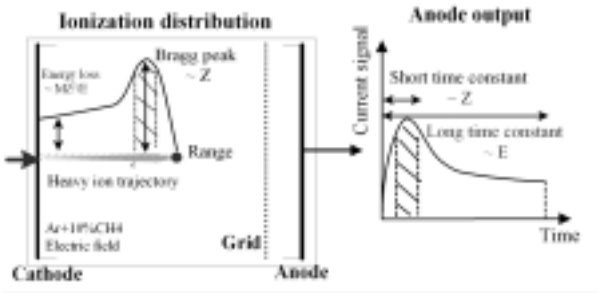


Fig. 1 Detection scheme of BCS method

To decrease the lower limit of the detection energy, BCS was improved at the part of entrance window. We use an aluminized Mylar film (2.5 μm thick) supported by tungsten wire to act as not only entrance window but also as a cathode electrode simultaneously. With the BCS developed, the new measurements of proton-induced reaction were performed using the AVF cyclotron at National Institute of Radiological Science (NIRS).

The experimental apparatus shown in Fig.2 is almost the same as one employed in the previous measurement. The fragments emitted to 30 degree direction were measured. The proton energy was 70 MeV. Proton beam current was ~10 nA. For samples, foils of aluminum 2 μm thick and polypropylene 4 μm thick were employed. In the measurement circuit, the energy signal and the Bragg peak signal were obtained from the anode signal by shaping with a long time constant (6 μsec) and a short time constant (0.25 μsec), respectively. To reduce background events and dead time of ADC, only coincidental events between anode and cathode were accumulated. The resolving time is set to 6 μsec that is equivalent to the maximum traveling time of electrons from the cathode to the grid. They are collected as a two-dimensioned data using KODAQ handler [8] with CAMAC system.

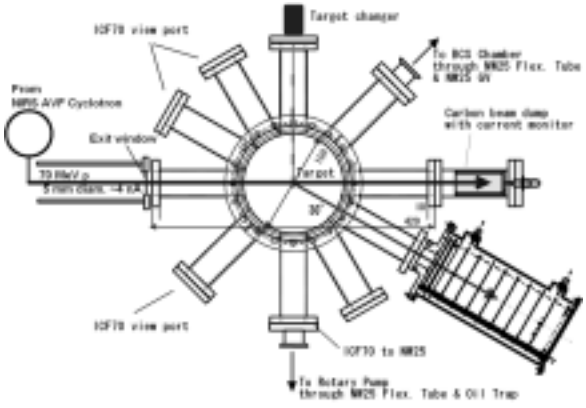


Fig2. Experimental setup of BCS in proton-induced reaction

Figures 3 and 4 show the measured two-dimensional spectra on the energy *vs.* Bragg peak of fragments from 4 μm thick polypropylene and 2 μm thick aluminum, respectively. Excellent separation of each fragment and S/N ratio are confirmed up to Z = 6 (Carbon), 9 (Fluorine) for polypropylene and aluminum sample, respectively, in the energy region where particles are separated by the difference of Bragg peak value. In case of aluminum sample, fragments heavier than fluorine could not be identified because these heavier products have too low energy to make ionization shape of Bragg peak and detected mainly below limit of identification using Bragg peak. The turning blows at maximum energy point in fig. 3 and 4 are caused by the fragments that have ranges longer than the cathode-grid distance which is the active region. It is meaningful to extend the measurable energy range by developing a correction method for this effect from the information of the energy deposit (ΔE).

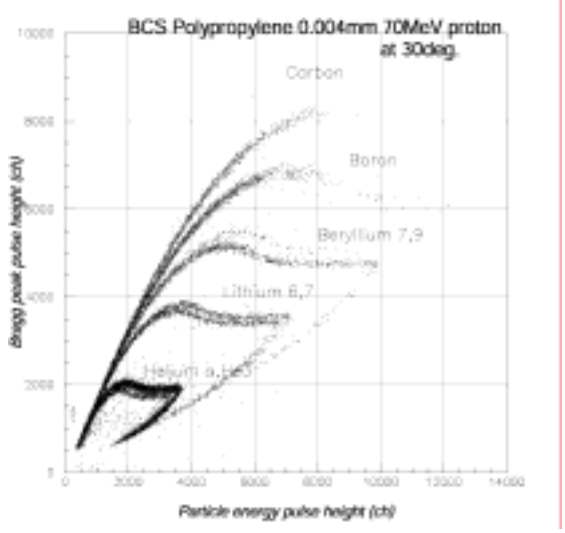


Fig.3 energy *vs* Bragg peak two-dimensional spectra for polypropylene 4 μm thick sample

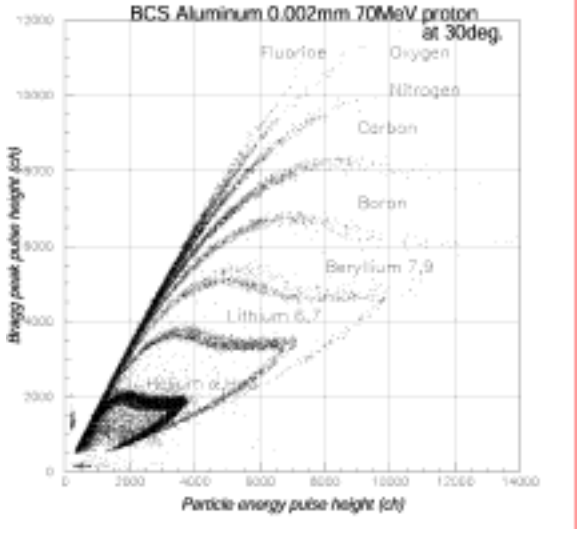


Fig.4 energy *vs* Bragg peak two-dimensional spectra for aluminum 2 μm thick sample

**3. ENERGY TIME-OF-FLIGHT METHOD (E-TOF)**

BCS method has several difficulties to cover whole energy region of fragment. We are developing to do fragment measurement for proton-induced reactions using an Energy Time-Of-Flight (E-TOF) method which is used in heavy ion detection. In this method, the energy and TOF of the fragment is measured and mass number is derived by combing the energy and TOF information. Therefore, the dynamic range of fragment energy is higher than in BCS. These data will be useful to complement data obtained with BCS.

The measurements of proton-induced reaction with E-TOF method were done also using AVF cyclotron at NIRS. The schematic view of the experimental setup is shown in Fig.5. The fragments emitted to 30 degree direction were measured. The proton energy was 70 MeV and beam current was ~10 nA, For samples, foils of aluminum 2 μm thick, and polypropylene 4 μm thick were employed similarly to the case of BCS.

It is difficult to obtain sufficient beam current (more than 10 nA) and time resolution of a beam burst (less than 1 nsec), concurrently. Therefore we use a thin detector in place of the RF signal from the cyclotron, to obtain timing signal of fragments for TOF. For a start detector of TOF, we employed an Ultra-thin plastic scintillator (Pilot-B: 5 μm thick) which had good time resolution and low energy loss for fragments. For a stop detector (E detector), a Silicon Solid State Detector (SSD) with good energy

resolution was adopted. The flight path is ~1.0 m. The scattering chamber was designed to enable simultaneous measurements of BCS and E-TOF. The combination of these methods would be powerful for the measurement of fragments induced by charged particles.

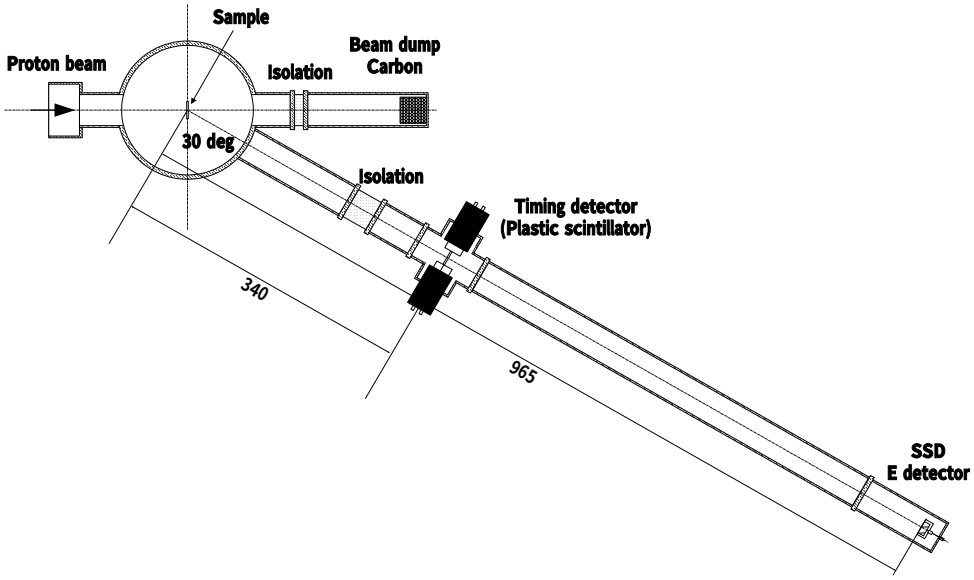


Fig.5 Schematic view of experimental setup for E-TOF measurement

Up to now, we identified the fragments from polypropylene (4 μm thick) up to A=12 with the measurement system using an ultra-thin plastic scintillator and SSD with a 0.965 m flight path as shown in fig.6. The energy spectra of fragments above mass of 6 were measured on the almost whole energy range. The fragments of mass number 5, 8, 9 were very few and the fragments above mass number 10 have very small energy. The time resolution of this setup was not good enough because we use SSD for a timing detector too. We will improve the measuring system by using two timing detectors for TOF measurement (start and stop signals) in the near future.

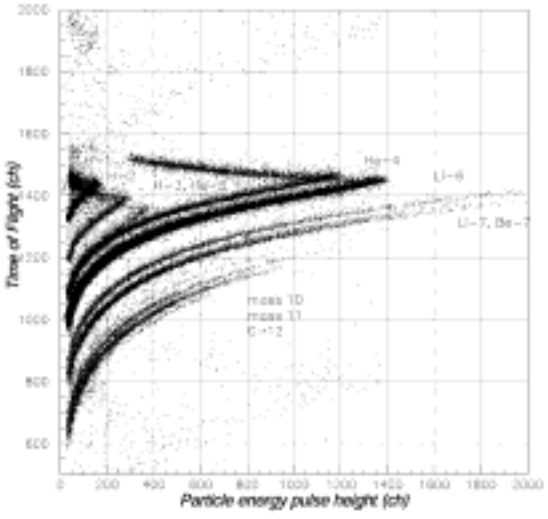


Fig.6 The energy *vs* TOF two-dimensional spectrum for carbon 100 μm thick sample

## 4. RESULTS OF FRAGMENT PRODUCTION CROSS-SECTION

The energy spectra of fragment heavier than alpha particle were obtained by both methods of BCS and E-TOF. Figure 7 shows the energy spectra of α-particle emitted to 30 degree from carbon and aluminum which were obtained with the BCS and E-TOF method. As shown in Fig.7, the data obtained with BCS and E-TOF method are consistent with each other in the overlapping region. The result of α-particle shows good agreements with LA150 [9] except for the case of aluminum above 10 MeV. Figure 8 shows the lithium spectra obtained with the BCS method. The data is compared with the previous data [4], QMD calculation with PHITS code [10] and LA150 [9]. The present data was obtained over wider energy range compared with previous one. The previous data have uncertainty due to the energy loss correction. The QMD calculation with the PHITS code show better agreement with the present one than LA150. Further, LA150 treats the angular distribution of fragment heavier than alpha particle as isotropic. Figure 9 and 10 show the energy spectra of fragments with mass number 6 and 7, respectively, obtained with E-TOF method. The present data for the mass number 6 agree with the PHITS, but not with LA150. For mass = 7, there are the experimental data by C. T. Roche et al [3]. but these data is obtained by incident energy of 45 MeV and 100 MeV. Present data agree well with the data by Roche et al. in the shape. PHITS and LA150 underestimate present data in the higher energy region.

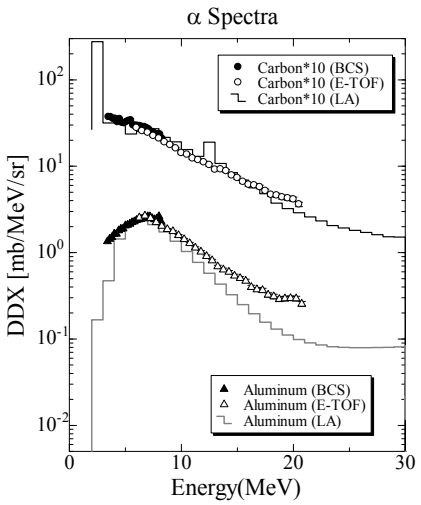


Fig.7 alpha spectra

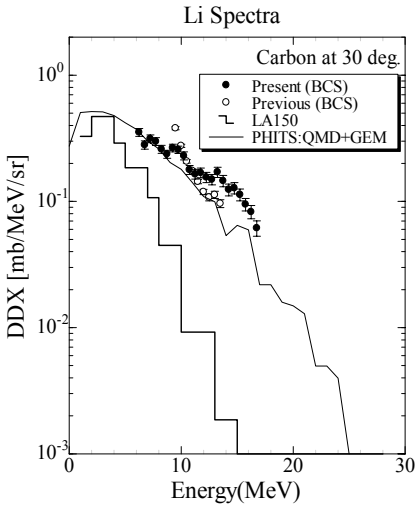


Fig.8 lithium spectra

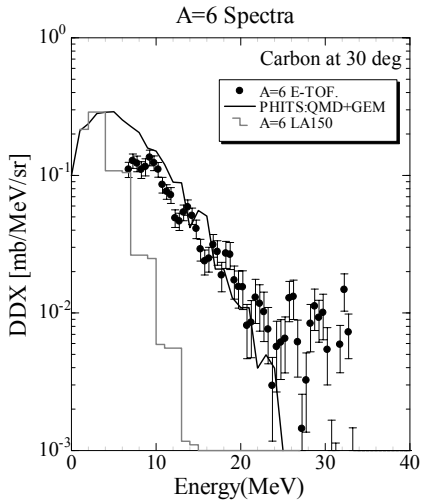


Fig.9 mass 6 spectra

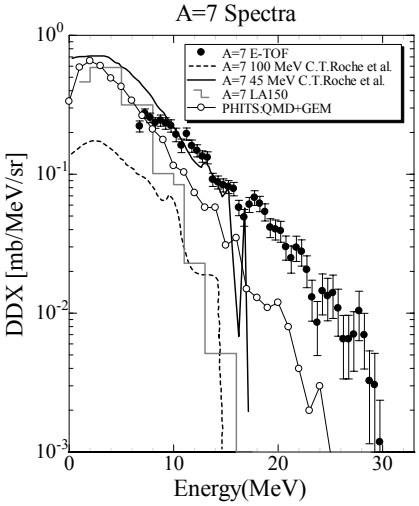


Fig.10 mass 7 spectra

## 5. SUMMARY

We developed a BCS detector and E-TOF method aiming at measurement of fragment production cross section for proton-induced reactions. For BCS, excellent separation of each fragment is confirmed up to Z = 6 (Carbon), 9 (Fluorine) for polypropylene and aluminum samples, respectively. For E-TOF, we could identify the fragments from polypropylene (4 μm thick) up to A=12 using an ultra-thin plastic scintillator for the start detector and SSD for the stop detector with ~1 m flight path. The data obtained with both methods were consistent with each other. The new results were obtained for fragment heavier than α-particle and compared with LA150 data library, QMD calculation in the PHITS code. The LA150 data agrees with the present data for α-particle but show much underestimation for fragment heavier than lithium. For fragment, QMD calculation is better than LA150 but underestimates the experimental data generally.

In the near future, we will improve the measuring method with the following refinements and the data will be applied for the analysis of SEU and dose contributions:

1) extension of the dynamic range for BCS and
2) enlarge the detection solid angle for E-TOF

For 1) we will put SSD detector backward anode electrode to detect the high energy fragments that have ranges longer than the cathode-grid distance. For 2) we will put the start detector to sample to enlarge the detection solid angle.


## ACKNOWLEDGEMENT

The authors express their thanks to the operation crew of the NIRS cyclotron for their cooperation.


## REFERENCES


[1] C.R.Gruhn, M.Binimi, R.Legrain, R.Loveman, W.Pang, M.Roach, D.K.Scott, A.Shotter, T.J.Symons, J.Wouters, M.Zisman, R.Devries, Y.C.Peng and W.Sondheim, *Nucl. Instrum. Methods*, **196** (1982) 33

[2] N.J.Shenhav and H.Stelzer, *Nucl.Instrm.Meth.* **228** (1985) 359

[3] C.T.Roche, R.G.Clark, G.J.Mathews and V.E.Viola, Jr, *Phys. Rev. C* **14** (1976) 410

[4]M. Hagiwara, T. Sanami, M.Baba, T. Oishi, M.Takada, H. Nakashima and S.Tanaka, Proc. of *Nucl. data.Sym.* (2003)

[5] T. Sanami, M. Baba, M. Hagiwara, T.Hiroishi, M.Hosokawa, N.Kawata, N.Hirabayashi, T.Oishi, H.Nakashima and S.Tanaka. *J. Nucl. Sci. and Tech.* **Suppl. 4** (2004) 502

[6] T.Sanami, M.Baba, K.Saito, N.Hirakawa. *Nucl. Instrum. Meth. A***440** (2000) 403

[7] O.Bunemann, T.E. Cranshaw, J.A. Harvey, Can. *J. Res. A***27** (1949) 373

[8] K.Omata and Y.Hujita, INS-Rep-884, Institute for Nuclear Study, University of Tokyo, 1991

[9] M. B. Cadwick, P. G.Young, S. Chiba, S.C. Frankle, G. M. Hale, H. G. Hughes, A. J. Koning, R. C. Little, R. E. MacFarlane, R. E. Praeel and L.S. Waters, *Nucl. Sci. Eng.*, **1331** (1999) 293

[10] H. Iwase, K. Niita, T. Nakamura, *J. Nucl. Sci. and Tech.* **39** No.11 (2002) 1142